Journal of Colloid and Interface Science 451 (2015) 40–45

Contents lists available at ScienceDirect

Journal of Colloid and Interface Science

www.elsevier.com/locate/jcis

Preparation of efficient cadmium sulfide nanofibers for hydrogen production using ethylenediamine ($NH_2CH_2CH_2NH_2$) as template

Agileo Hernández-Gordillo [a,*,1], Socorro Oros-Ruiz [b,1], Ricardo Gómez [b]

[a] Instituto de Investigaciones en Materiales, Universidad Nacional Autónoma de México, Circuito Exterior SN, Ciudad Universitaria, CP 04510 México, D.F., Coyoacán, Mexico
[b] Universidad Autónoma Metropolitana-Iztapalapa, Depto. de Química, Área de Catálisis, Grupo ECOCATAL, Av. San Rafael Atlixco No 186, México, D.F. 09340, Mexico

GRAPHICAL ABSTRACT

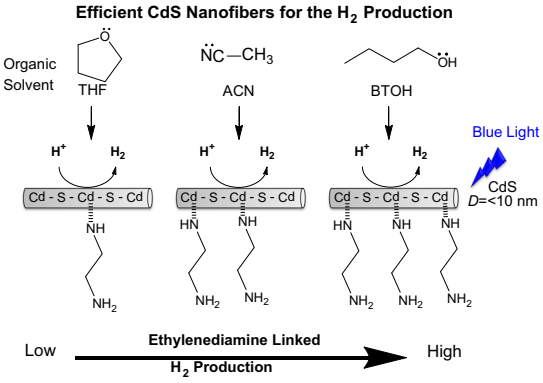

ARTICLE INFO

Article history:
Received 4 February 2015
Accepted 27 March 2015
Available online 3 April 2015

Keywords:
CdS nanofiber
Ethylenediamine template
H_2 production
Visible light irradiation

ABSTRACT

The preparation of CdS was performed by the precipitation method using ethylenediamine as template and tetrahydrofuran, acetonitrile or butanol as organic solvents. The formation of CdS with hexagonal structure was observed by XRD due to the template effect. FTIR studies showed that the amount of the template linked to the surface of the CdS depends on the organic solvent used. TEM observations evidenced the formations of CdS nanofibers and the EDS analysis show the chemical composition of the surface. The photocatalytic activity of CdS nanofibers under blue light irradiation was strongly influenced by the amount of ethylenediamine template on the nanofiber surface. It was observed that when the amount of the template on the samples diminishes by the heat treatment, the photocatalytic activity is affected. The role of the ethylenediamine template in the mechanism for the H_2 production reaction is discussed.

1. Introduction

Cadmium sulfide semiconductors have been one of the most used photocatalysts for redox reactions. For photocatalytic hydrogen production, it is an appropriate semiconductor since CdS have favorable negative conduction band respect to the redox potential of the H^+/H couple [1,2], and because of its narrow band-gap energy (2.4 eV) allows the absorption of visible light and perform the reduction of protons (H^+) during the water splitting [3–6]. However, to obtain a good photocatalytic efficiency, CdS should be highly crystalline in hexagonal phase with nanostructured morphologies of nanorods, multiarmed nanorods [7,8], nanowires [9] or nanofibers [10], and they should possess a high specific surface

* Corresponding author.
E-mail addresses: agileo12@hotmail.com, agileohg@iim.unam.mx (A. Hernández-Gordillo).
[1] Cátedras-CONACYT.

http://dx.doi.org/10.1016/j.jcis.2015.03.052
0021-9797/

area in order to increase the H_2 production. To obtain these nanostructured CdS, several methods are used, including ultrasonic microemulsion [11–14], hydrothermal or solvothermal methods [15]. It has been reported that the synthesis parameters such as molar ratio, precursor source and the template used such as 2-mercaptoethanol, methionine, glutathione [16], ethylenglicol [17] and *n*-butanol [18] have important effects on the physicochemical properties on the semiconductor. When the solvothermal method is used, the diamine organic molecules act as ligand agent modifying the nanostructured CdS surface [16–19]. Among the amine ligands, there are triethanolamine [8], dodecylamine [20], triethylene tetramine [21] or ethylenediamine [22–25]; however, they can also be combined with other organic molecules in aqueous solutions, performing the synthesis in binary systems [26–30]. Typically, the ethylenediamine ligand acts as a cation sequestrant binding to the Cd^{2+} ions on the CdS surface [22,31] creating sulfur vacancies (V^{+}_{s}). The superficial Cd^{2+} ions are much more efficient for the H_2 production than the superficial S^{2-} ions [32]. The Cd^{2+} ions surface states act as electron traps, promoting the separation of the charge carriers. Thus, the electrons are deeply trapped at the sulfur vacancy (V^{+}_{s}), located below the CdS conduction band [32,33].

Different systems like olive oil/1-butanol/water [34], cyclohexane/sodium dodecyl sulfonate (SDS)/pentanol [35], water–ethylenediamine–benzene or cyclohexane [36], have been used for the CdS preparation, however the synthesis of CdS nanofibers covered with ethylenediamine by using protic or aprotic polar solvent has not been yet explored.

In the present work, nanofibers of hexagonal CdS were synthesized by the precipitation method with a mixture of water/ethylenediamine/organic solvent. The effect of the organic solvent; *n*-butanol, acetonitrile or tetrahydrofuran used on the amount of the ethylenediamine linked on the superficial Cd^{2+} ions were investigated. The samples were evaluated for the photocatalytic reaction of H_2 production under blue light irradiation. The influence of the heat treatment (150 or 200 °C) on the photocatalytic activity of CdS nanofibers as a function of the template was also investigated.

2. Experimental section

2.1. Synthesis of the CdS nanofibers

The CdS nanofibers were prepared by the precipitation method [10] using a mixture containing 10 vol.% of H_2O, 60 vol.% of ethylenediamine (*EN*, Aldrich) and 30 vol.% of the organic solvent: tetrahydrofuran (Aldrich), acetonitrile (Aldrich) or *n*-butanol (Baker). In a typical procedure, appropriate amounts of $Cd(NO_3)_2H_2O$ (Reasol) were dissolved in the aqueous solutions of acetonitrile, tetrahydrofuran or *n*-butanol at room temperature at constant stirring for 15 min; then the *EN* was added. Afterward carbon disulfide (CS_2, Aldrich) was added drop wise, maintaining a stoichiometry molar ratio of S:Cd of 1:1. The obtained transparent solution was heated at boiling point (90–110 °C) under vigorous magnetic stirring for 1 h and subsequently cooled at room temperature. Finally, the resulting yellow precipitate was collected by filtration, washed with an ethanol–water solution and dried at 80 °C for 1 h. The final solids were labeled with the name of the organic solvent used as **ACN** for acetonitrile, **THF** for tetrahydrofuran and **BTOH** for *n*-butanol.

Separately, part of the CdS nanofibers dried at 80 °C, prepared in the water–*EN*–*n*-butanol solution, were heated at either 150 or 200 °C and then were labeled as **BTOH-1** and **BTOH-2**, respectively.

2.2. Characterization of the CdS nanofibers

The obtained nanostructured CdS were characterized by X-ray powder diffraction using a D8 Advance Bruker X-ray diffractometer with Cu Kα radiation of 1.5406 A (35 kV, 25 mA). The scanning range was between 10° and 70° (2 theta), and a step size of 0.03°/s. The morphology was determined using a transmission electron microscope (TEM) JEOL JEM 1230 operated at 100 keV. The specific surface area was calculated by the BET method, from the nitrogen adsorption–desorption isotherms obtained on a Quantachrome Autosorb-3B apparatus. Prior to N_2 admission in the cell, all the samples were degaussed at 80 °C under vacuum for 5 h. Diffuse reflectance spectroscopy was performed in the range of 190 and 600 nm, using a Varian Cary-100 spectrometer equipped with an integration sphere. The band-gap energy of the semiconductors (*Eg*) was calculated using the Kubelka–Munk method. The semiquantitative chemical composition of the CdS nanofibers was revealed by field emission scanning electron microscopy (FESEM) using a Helios NanoLab 600i equipped with Advanced DualBeam coupled with an EDS (energy dispersive X-ray spectroscopy) detector. The nanofibers samples were deposited on copper ribbon to avoid the carbon interference.

2.3. FTIR spectroscopy of the CdS surface

The FTIR absorption spectra of all the samples were recorded on a Shimadzu IR-440 FTIR spectrometer using an attenuated total reflection (ATR) accessory provided of a ZnSe crystal. After each measurement, the crystal was cleaned with ethanol before loading the next powder and the pressure used was of 815 Psi of pressure. Typically, 200 scans at a resolution of 8 cm^{-1} in the range between 500 cm^{-1} and 4000 cm^{-1} in the transmittance mode were used for the measurements at room temperature.

3. Results

3.1. Crystalline structure of CdS

The X-ray diffraction patterns of the CdS semiconductors (Fig. 1) exhibit reflection peaks corresponding to the main planes (100), (002) and (101), which were indexed to the hexagonal phase of CdS (JCPDS No. 41-1049), with lattice parameters (a = 4.1 and c = 6.7 Å) close to the data values reported for CdS [9,29]. However, for the **BTOH** sample, the lattice parameters were smaller (Table 1), suggesting slight contractions in the hexagonal structure. The relative ratio intensity of the (110) and (103) planes for all the CdS materials was 0.94, suggesting that its crystalline structure is purely hexagonal [1]. The high relative intensity of the (002) reflection peak of the CdS is indicative of the preferential growth along the *c*-axis of the hexagonal phase [20]. The average nanocrystallite size for all the hexagonal CdS by using the Debye-Scherrer equation from the diffraction peaks of the (002) plane is above 9 nm, being the smallest nanocrystallite size for the **BTOH** sample (5.6 nm). The hexagonal structure of CdS was obtained by the effect of the ethylenediamine template.

3.2. Morphology of the nanocrystalline CdS

It is known that the morphology of the nanostructured materials strongly depends on the physicochemical properties of the template and the solvents used (dielectric constant, dipole momentum, hydrogen binding, Table 1). In our CdS materials prepared by using different solvents, the resulting morphology observed by TEM images exhibited flexible fibers-like morphologies (Fig. 2a–c), with

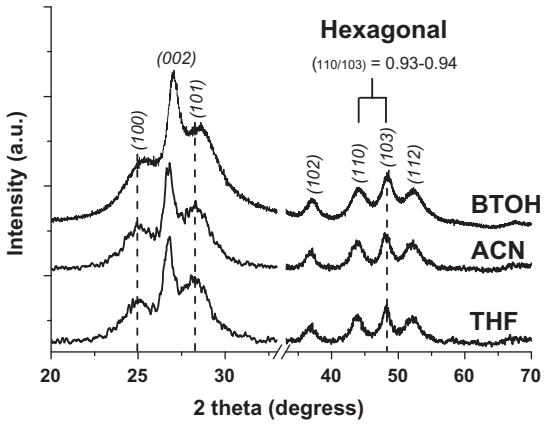

Fig. 1. X-ray diffraction patterns of CdS prepared in tetrahydrofuran (**THF**), acetonitrile (**ACN**) and butanol (**BTOH**) solvent.

Table 1
Data of the physicochemical properties of each solvent.

Solvent	Dielectric constant	Dipole momentum (*Debyes*)	Hydrogen-P	Classification
THF	7.4	1.7	23	Aprotic (—O:)
ACN	37.5	3.5	16	Aprotic (═N:)
BTOH	17	1.7	43	Protic (:O—H)
EN	13	1.9	–	Protic (:N—H)
H_2O	78.5	1.8	58	Protic (:O—H)

diameters (*D*) ranging from 4 to 15 nm. The obtained nanofibers could be related to the interaction between CS_2, Cd[*EN*]$^{2+}$ complex with the organic solvent. It is known that when the Cd^{2+} ions are in contact with the *EN* template in aqueous solution, they form the characteristic Cd[*EN*]$^{2+}$ complex, while the CS_2 reacts with the *EN* template, forming a polymerized product **[±HNCH$_2$CHNHCS±]*n*** and then the S^{2+} ions are simultaneously released [11–14]. In this case, the polymerized product **[±HNCH$_2$CHNHCS±]*n*** contains a hydrophobic and a hydrophilic group [30], which may interact in a different manner depending on the hydrogen binding capacity with the aprotic polar solvent (acetonitrile or tetrahydrofuran) or with the protic polar solvent (*n*-butanol). Finally, the formed S^{2+} ions react with the Cd[*EN*]$^{2+}$ complex in the solvent mixture system to form CdS(*EN*)$_{0.5}$ nanofibers. Simultaneously, the nanofibers could become to hexagonal CdS, where part of *EN* ligand could remain preferentially linked to the superficial Cd^{2+} ions [8]. Since these fibers are agglomerated, the determination of length (*L*) was difficult, but probably varying between 100 and 500 nm. This result suggests that the formation of flexible nanofibers of CdS was successfully achieved using different organic solvents. CdS nanofibers are more agglomerated when they are prepared in acetonitrile than those prepared in tetrahydrofuran or in *n*-butanol.

3.3. Textural properties of CdS nanofibers

The nitrogen adsorption–desorption isotherms of CdS nanofibers are shown in Fig. 3A. The hysteresis loop at a high relative pressure (0.8–0.9 P/P_0), suggest the presence the mesoporous structure up to 25 nm, as is shown in the pore size distribution (Fig. 3B), where the pore diameter is centered in 30 nm. Considering that the diameter of nanofiber particle is between 4 and 15 nm (Fig. 2), the pores are owing to interstitial spaces between fibers-fibers nanoparticles (interparticle porosity) [37]. According to the IUPAC classification they exhibit type II isotherms, which are characteristic of materials where the interactions between the adsorbate and the adsorbent is weak. The specific surface areas of the CdS samples were determined from the N_2 adsorption isotherms and the obtained values were between 125 and 152 m^2/g (Table 2).

3.4. FTIR spectroscopy of EN absorbed on CdS nanofibers

FTIR spectra of the CdS nanofibers (Fig. 4) exhibited bands at 3424 cm^{-1} associated to the stretching vibration of the hydroxyl (O—H) bond, however, it is overlapped with the band at 3266 cm^{-1} corresponding to the stretching vibrations of N—H bond of the ethylenediamine template. Therefore, all the CdS nanofibers show the presence of hydroxyl groups on its surface [31]. The bands at 2952, 1584, 1324 and 1007 cm^{-1} are associated to the stretching vibrations of C—H, —NH_2, and C—N bonds, respectively, for the diamine template, which are originated from the Cd(*EN*)$^{2+}$ complex, where the ethylenediamine molecule uses a *trans*-conformation to coordinate with superficial Cd^{2+} ions on the CdS nanofibers [38,39]. Depending on the organic solvent used for the preparation of the CdS nanofibers, these bands vary in transmittance, being more pronounced in **BTOH** sample, suggesting that more ethylenediamine is favorably linked to the superficial Cd^{2+} ions of the (1 0 0) and (0 1 0) planes [8], in the presence of *n*-butanol (Fig. 3b). For all the CdS nanofibers, the sharp band at 629 cm^{-1} is associated to the Cd—S bond [36–40], however, it is expected that the CdS covered with ethylenediamine may be rich in both superficial Cd^{2+} ions and sulfur vacancies (V^{s+}) [32]. In addition, a vibration band at 1098 cm^{-1} varies in transmittance depending of the organic solvent, which it is the highest for THF sample and it is the lowest for the BTOH sample. These signals could be associated

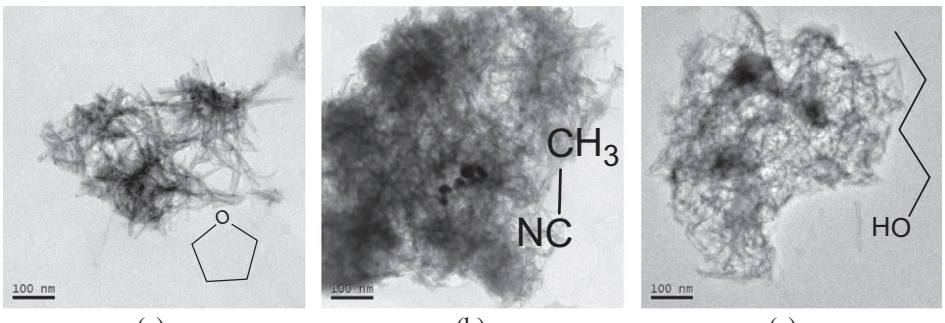

Fig. 2. TEM images of the CdS nanofibers synthesized in a mixture system of water–ethylenediamine–organic solvent: (a) tetrahydrofuran, (b) acetonitrile and (c) butanol.

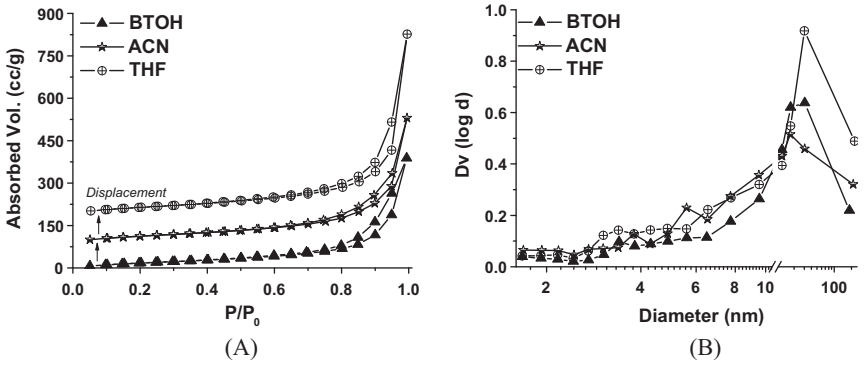

Fig. 3. (A) N_2 adsorption–desorption isotherms and (B) pore size distribution of the CdS nanofibers.

Table 2
Data of lattice parameter, crystallite size, band gap energy and specific surface area for CdS nanofibers.

Sample	Lattice parameter *a* (Å) and *c* (Å)		Crystallite Size 002 plane (nm)	S_g (m^2/g)	E_g (eV)
THF	4.15	6.67	8.4	152	2.59
ACN	4.16	6.68	8.4	144	2.58
BTOH	4.04	6.60	5.6	125	2.65
BTOH-2	4.15	6.78	5.5	125	2.40

Table 3
Data of chemical composition from EDS analysis of CdS nanofibers and the experimental molar atomic ratio of S/Cd, O/Cd, N/Cd.

Sample	Weight composition (%)					Molar atomic ratio			
	Cd	S	O	N	C	S/Cd	O/Cd	N/Cd	N/C
THF	36.54	10.19	8.23	4.5	40.55	0.97	1.58	0.98	0.12
ACN	43.84	11.34	9.99	6.0	34.11	0.95	1.60	1.20	0.15
BTOH	40.06	11.04	9.89	7.18	31.84	0.96	1.73	1.44	0.16
BTOH-2	44.57	12.25	8.42	3.8	30.96	0.97	1.65	0.68	0.10

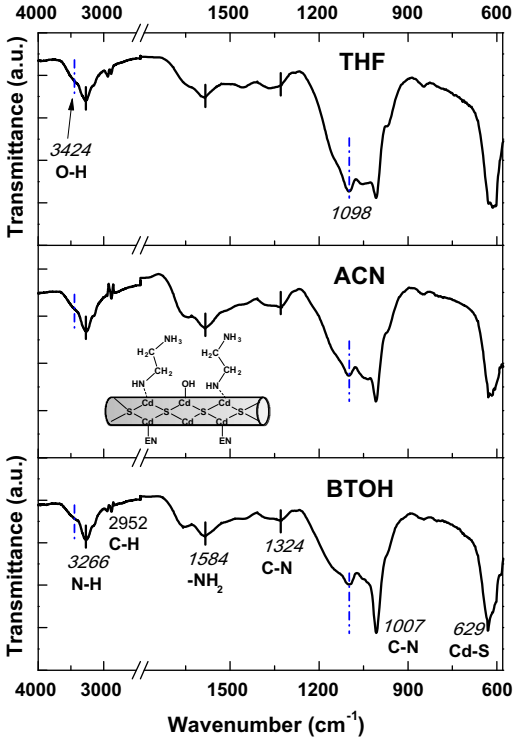

Fig. 4. FTIR spectra of CdS nanofibers synthesized in tetrahydrofuran (**THF**), acetonitrile (**ACN**) and butanol (**BTOH**). A representation of the ethylenediamine linked on the nanofibers surface of hexagonal CdS is inset.

the presence of residual compounds of the secondary reactions occurred during the synthesis.

3.5. EDS composition of CdS nanofibers

The CdS nanofibers are composed of cadmium and sulfur (Table 3); however, the EDS spectrum (S1 in Supplementary Information) exhibits additional oxygen, nitrogen and carbon peaks. According to the experimental molar atomic ratio value of the S/Cd, all synthesized CdS nanofibers (~0.95–97), are close to the theoretical ratio of S/Cd = 1, indicating that the similar amount of sulfur defects is present on the CdS surface [41]. The molar atomic ratio of O/Cd and N/Cd are slightly higher for the CdS prepared in *n*-butanol (BTOH) than that for the one obtained using tetrahydrofuran as solvent. This oxygen is related to the CO_2 formation on the CdS surface provided by the CS_2 decomposition [42]. On the other hand the high molar atomic ratio of N/C for the BTOH sample could be related to the high content of the ethylenediamine template.

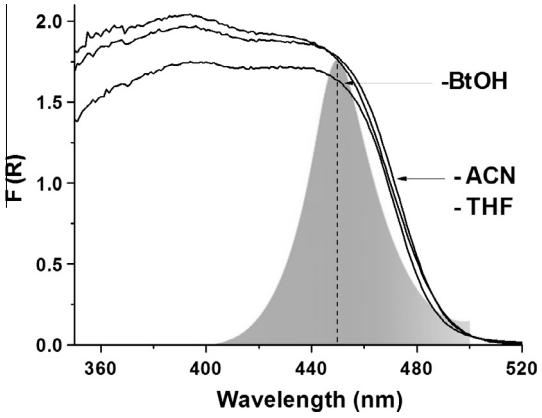

Fig. 5. UV–Vis diffuse reflectance spectra for the CdS nanofibers synthesized in tetrahydrofuran (**THF**), acetonitrile (**ACN**) and butanol (**BTOH**) solvent.

3.6. Optical blue-absorption of CdS nanofibers

UV–Vis diffuse reflectance spectra for the CdS nanofibers (Fig. 5) exhibit similar absorption edges in the visible light region close to 460–490 nm, attributed to the intrinsic band-gap transition of electrons from the valence band to the conduction band

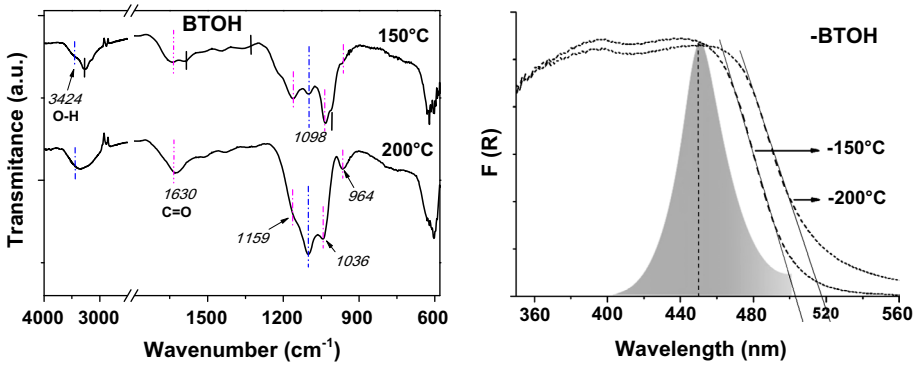

Fig. 6. (A) FTIR spectra and (B) UV–Vis diffuse reflectance spectra of the CdS nanofibers prepared in butanol solvent and heated at 150 and 200 °C.

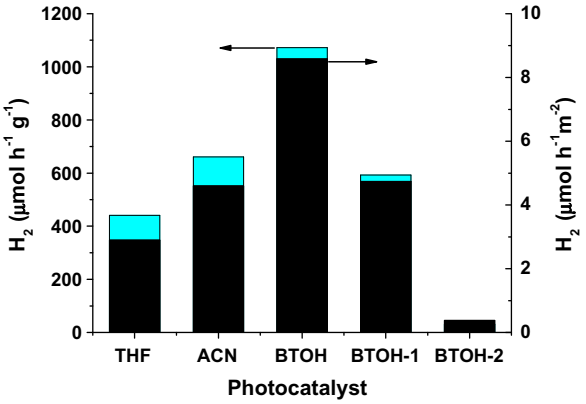

Fig. 7. Comparison of the H_2 production rate from methanol–water solution for the CdS nanofibers photocatalysts under blue light irradiation. The H_2 production rate was also standardized as a function of specific surface area. (For interpretation of the references to colour in this figure legend, the reader is referred to the web version of this article.)

[9]. The shaded area in Fig. 4 corresponds to the emission spectrum of the blue LED lamp used for its activation. The band-gap energies (~2.58–2.65 eV, Table 2) were estimated by the Kubelka–Munk (K–M) method (linear plot $(FR \times h\nu)^2$ vs $h\nu$), the marked blue shift of the absorption edge (2.65 eV) can be due to the quantum confinement effect [22,23,29]. In addition, the *EN* linked of the nanofibers can passivate the semiconductor surface by quenching the number of surface states. Increasing the energy between the surface states modifies the absorption edge and a blue-shift was produced by the presence of sulfur vacancies (V^{s+}) [16,43].

3.7. Surface modification of CdS nanofibers

In order to study the stability on CdS surface, heat treatments (150 and 200 °C) were applied to the samples. The X-ray diffraction for BTOH-2 treated at 200 °C (not shown) exhibited the same diffraction peaks corresponding to the hexagonal structure of CdS, however, the lattice parameter for the CdS was close to the data values reported for the bulk CdS. The crystallite size was similar than the one obtained for CdS dried at 80 °C (5.6 nm, Table 2). It is known that the increasing of the heat treatment induces changes in the structure, decreasing structural defects (anionic or cationic) in the material [44]. Thus, the changing in the lattice parameter suggests that the sulfur defects (V^{s+}) were probably eliminated. To confirm this asseveration, the CdS heated at 150 and 200 °C

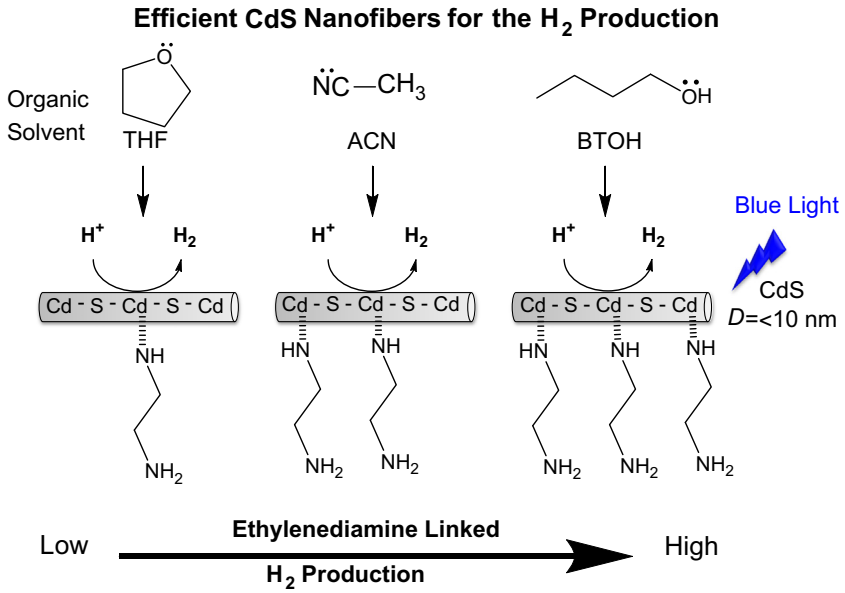

Fig. 8. Schematic representation of the CdS nanofibers with different amounts of *EN* adsorbed on superficial Cd^{2+} ions synthesized in different solvents: tetrahydrofuran (**THF**), acetonitrile (**ACN**) and butanol (**BTOH**), for H_2 production under blue light irradiation. (For interpretation of the references to colour in this figure legend, the reader is referred to the web version of this article.)

were analyzed by FTIR spectroscopy (Fig. 6A). For BTOH-1 heated at 150 °C, the vibration bands of C—H, N—H, NH_2, C—N bonds remain unaltered, whereas new vibration bands in the intervals from 1150 to 960 cm^{-1} assigned to the residual products of secondary reactions appear. When BTOH sample was heated at 200 °C, these vibration bands corresponding to ethylenediamine template were not observed due to the desorption of *EN* molecule which was linked on the surface. The elimination of *EN* induces changes in the structural surface and as a consequence a decreasing of the sulfur vacancies [45]. According to the EDS analysis, the low molar atomic ratio of N/C = 0.10 for the BTOH-2 sample (Table 2), suggests a decreasing in the nitrogen contents on the CdS surface. These modifications were reflected in the optical-electronic properties of the CdS (Fig. 6B), where the absorption edge was red-shifted as the structural defects were originated by increasing the heat treatment. The estimated band gap energy was 2.4 eV, which is characteristic of bulk CdS free of sulfur vacancies.

3.8. Photocatalytic activity of CdS nanofibers

The evolved H_2 from methanol–water solution under blue light irradiation using CdS nanofibers, shows correlations between the amount of *EN* linked to the nanofibers surface and the photocatalytic activity (Fig. 7), where the **BTOH** sample with the highest amount of ethylenediamine linked to its surface is the more active (1072 μm h^{-1} g^{-1}). On the other hand, **THF** had a negative effect on the photocatalytic activity, producing 441 μm h^{-1} g^{-1} of H_2. In addition, the standardized H_2 produced as a function of the specific surface area showed that the specific surface area was not determined to achieve a high H_2 evolution.

In order to study the stability and the effect of the *EN* linked on the nanofibers surface, the evolution of H_2 of the BTOH samples heated at 150 and 200 °C are shown in Fig. 7 (**BTOH-1** and **BTOH-2**). The H_2 production rate decreased when the BTOH sample was treated at 150 °C, until to its complete inhibition when the sample was treated at 200 °C. Despite the specific surface area was unaltered (125 m^2/g, Table 2), at different heat treatments, the loss of photoactivity was due to the *EN* elimination on the CdS surface. Thus, the photocatalytic activity strongly depends on the presence of the *EN* on the nanofibers surface (Fig. 8). Considering that the *EN* is linked on the superficial Cd^{2+} ions, creating surface states, the blue-photogenerated electrons in the semiconductor are trapped in these surface states, prolonging the lifetime of the electrons, which are transferred to the protons to produce H_2 and promoting the electron–hole separation.

4. Conclusions

Nanostructured CdS nanofibers were successfully obtained with ethylenediamine template in different organic solvents (tetrahydrofuran, acetonitrile or *n*-butanol) by the simple precipitation method. The CdS nanofibers exhibited hexagonal structure, optical absorption in the blue region and similar specific surface areas; however the synthesis of these nanofibers in different organic solvent induced different amounts of the ethylenediamine linked to the CdS surface. The amount of template was affected by the heat treatment, where at 200 °C the ethylenediamine was completely eliminated. The highest H_2 production under blue light irradiation was obtained by the CdS nanofibers prepared using *n*-butanol as organic solvent, and it was attributed to the presence of ethylenediamine linked to the superficial Cd^{2+} ions.

Acknowledgments

This research was made with the support of CONACYT-SEP CB-2010-01 157156 and FOINS/75/2012c project Artificial Photosynthesis. Agileo Hernández-Gordillo thanks to CONACYT for financial support through the Cátedras-Conacyt/1169 project.

Appendix A. Supplementary material

Supplementary data associated with this article can be found, in the online version, at http://dx.doi.org/10.1016/j.jcis.2015.03.052.

References

[1] D. Lang, Q. Xiang, G. Qiu, X. Feng, F. Liu, Dalton Trans. 43 (2014) 7245.
[2] X. Li, J. Yu, J. Low, Y. Fang, J. Xiaoc, X. Chen, J. Mater. Chem. A 3 (2015) 2485–2534.
[3] C. Li, J. Yuan, B. Han, W. Shangguan, Int. J. Hydrogen Energy 36 (2011) 4271–4279.
[4] Q. Xiang, B. Cheng, J. Yu, Appl. Catal. B: Environ. 138–139 (2013) 299–303.
[5] S. Chen, X. Chen, Q. Jiang, J. Yuan, C. Lin, W. Shangguan, Appl. Surf. Sci. 316 (2014) 590–594.
[6] H. Wang, W. Chen, J. Zhang, C. Huang, L. Mao, J. Hydrogen Energy 40 (2015) 340–345.
[7] J. Yu, Y. Yu, B. Cheng, RSC Adv. 2 (2012) 11829–11835.
[8] J. Yu, Y. Yu, P. Zhou, W. Xiao, B. Cheng, Appl. Catal. B: Environ. 156–157 (2014) 184–191.
[9] J. Jin, J. Yu, G. Liu, P.K. Wong, J. Mater. Chem. A 1 (2013) 10927–10934.
[10] A. Hernandez-Gordillo, F. Tzompantzi, S. Oros-ruiz, L.M. Torres-Martinez, R. Gómez, Catal. Commun. 45 (2014) 139–143.
[11] J. Huang, Y. Xie1, B. Li, Y. Liu, J. Lu, Y. Qian, J. Colloid Interface Sci. 236 (2001) 382–384.
[12] Y.-T. Chen, J.-B. Ding, Y. Guo, L.-B. Kong, H.-L. Li, Mater. Chem. Phys. 77 (2002) 734–737.
[13] X. Fu, D. Wang, J. Wang, H. Shi, C. Song, Mater. Res. Bull. 39 (2004) 1869–1874.
[14] N. Ghows, M.H. Entezari, Ultrason. Sonochem. 18 (2011) 269–275.
[15] Y. Li, Y. Hu, S. Peng, G. Lu, S. Li, J. Phys. Chem. C 113 (2009) 9352–9358.
[16] P. Thangadurai1, S. Balaji, P.T. Manoharan, Nanotechnology 19 (2008) 435708.
[17] S. Zhong, L. Zhang, Z. Huang, S. Wang, Appl. Surf. Sci. 257 (2011) 2599–2603.
[18] M. Ge, Y. Cui, L. Liu, Z. Zhou, Appl. Surf. Sci. 257 (2011) 6595–6600.
[19] A. Samadi-maybodi, F. Abbasi, R. Akhoondi, Colloids Surf. A: Physicochem. Eng. Aspects 447 (2014) 111–119.
[20] X. Wang, Z. Feng, D. Fan, F. Fan, C. Li, Cryst. Growth Des. 10 (12) (2010) 5312–5318.
[21] P. Dalvand, M.R. Mohammadi, D.J. Fray, Mater. Lett. 65 (2011) 1291–1294.
[22] X. Ma, F. Xu, Y. Liu, X. Liu, Z. Zhang, Y. Qian, Mater. Res. Bull. 40 (2005) 2180–2188.
[23] N.M.A. Hadia, S. García-Granda, J.R. García, J. Nanosci. Nanotechnol. 14 (2014) 5449–5454.
[24] Y-Jg Hsu, S-Y Lu, Y-F. Lin, Chem. Mater. 20 (2008) 2854–2856.
[25] H. Tang, M. Yan, H. Zhang, M. Xia, D. Yang, Mater. Lett. 59 (2005) 1024–1027.
[26] A. Vaneski, J. Schneider, A.S. Susha, A.L. Rogach, APL Mater. 2 (2014) 012104.
[27] D. Xu, Z. Liu, J. Liang, Y. Qian, J. Phys. Chem. B 109 (2005) 14344–14349.
[28] A. Phuruangrat, T. Thongtem, S. Thongtem, Curr. Appl. Phys. 9 (2009) S201–S204.
[29] I. Kazeminezhad, N. Hekmat, A. Kiasat1, Fibers Polym. 15 (4) (2014) 672–679.
[30] L. Huang, Y. Xie, B. Li, Y. Liu, Y. Qian, S. Zhang, Adv. Mater. 12 (2000) 808–811.
[31] S. Li, L. Zhang, T. Jiang, L. Chen, Y. Lin, D. Wang, T. Xie, Chem. Eur. J. 19 (19) (2013) 1–7.
[32] L. Huang, J. Yang, X. Wang, J. Han, H. Han, C. Li, Phys. Chem. Chem. Phys. 15 (2013) 553–560.
[33] G.Q. Xu, B. Liu, S.J. Xu, C.H. Chew, S.J. Chua, L.M. Gana, J. Phys. Chem. Solids 61 (2000) 829–836.
[34] M.E. EL-Hefnawy, Mod. Appl. Sci. 6 (4) (2012).
[35] M.Z. Rong, M.Q. Zhang, H.C. Liang, H.M. Zeng, Appl. Surf. Sci. 228 (2004) 176–190.
[36] Y. Xie, J. Huang, B. Li, Y. Liu, Y. Qian, Adv. Mater. 12 (20) (2000).
[37] D. Xie, Q. Su, Z. Dong, J. Zhang, G. Du, CrystEngComm 15 (2013) 8314.
[38] K. Krishsas, Asd-Robert.A. Plane, Inorg. Chem. 5 (59) (1966).
[39] P. Zhao, K. Huang, Cryst. Growth Des. 8 (2) (2008).
[40] S.K. Parayil, J. Baltrusaitis, C.-M. Wua, R.T. Koodali, Int. J. Hydrogen Energy 38 (2013) 2656–2669.
[41] P. Thangadurai1, S. Balaji, P.T. Manoharan, Nanotechnology 19 (2008) 435708–435716.
[42] L. Huang, J. Yang, X. Wang, J. Han, H. Han, C. Li, Phys. Chem. Chem. Phys. 15 (2013) 553–560.
[43] Q. Xiao, C. Xiao, Appl. Surf. Sci. 255 (2009) 7111–7114.
[44] V.B.K.A.M. Umarji, AIP Adv. 3 (2013) 082120.
[45] B.-J. Liu, T. Torimoto, H. Yoneyama, J. Photochem. Photobiol. A: Chem. 113 (1998) 93–97.